# On corner cutting in multi-obstacle avoidance problems

**Florin Stoican** * **Esten Ingar Grøtli** ** **Ionela Prodan** *** **Cristian Oară** *

* *Department of Automatic Control and Systems Engineering, UPB, Romania (florin.stoican@acse.pub.ro)*
** *Applied Cybernetics, SINTEF IKT, Norway (Esten Ingar.Grotli@sintef.no)*
*** *Laboratory of Conception and Integration of Systems (LCIS EA 3747), Grenoble INP, France (ionela.prodan@lcis.grenoble-inp.fr)*

**Abstract:** One challenging and not extensively studied issue in obstacle avoidance is the corner cutting problem. Avoidance constraints are usually imposed at the sampling time without regards to the intra-sample behavior of the dynamics. This paper improves upon state of the art by describing a multi-obstacle environment over a hyperplane arrangement scaffolding, provides a piecewise description of the "shadow" regions and represents them into a combined mixed integer and predictive control formulation. Furthermore, over-approximation constraints which reduce to strictly binary formulations are discussed in detail. Illustrative proofs of concept, comparisons with the state of the art and simulation results over a classical multi-obstacle avoidance problem validate the benefits of the proposed approach.

Keywords: Corner cutting problem, Hyperplane arrangement, Model Predictive Control (MPC), Mixed-Integer Programming (MIP), Multi-obstacle environment.

## 1. INTRODUCTION

Obstacle avoidance problems represent an active research topic due to both their wide applicability in practical settings and theoretical depths. The major issue is that the avoidance constraints lead to a feasible space which is non-convex and often non-connected. It is worth emphasizing that such an outcome is not just an artifact of the problem, but rather an intrinsic property which cannot be avoided.

The present paper concentrates on a particular issue: the *corner cutting problem* under a predictive control framework. Avoidance constraints are usually imposed at the sampling time without regards to the intra-sample behavior of the agent. This means that it is possible for an agent to "cut the corner" of an obstacle while apparently respecting the constraints. This is usually handled by changing the constraints to take into account the future position of the agent with respect to its current position. There are a variety of ways of implementing these requirements but they all seem (to the best of the authors' knowledge) to be conservative in their description Richards and Turnbull [2015], Maia and Galvão [2009], Deits and Tedrake [2015].

Here, we propose to use hyperplane arrangements as the main theoretical tool for constraint description. Namely, we partition the space into disjoint cells which can be either forbidden (the obstacles) or admissible (parts of the feasible space) and use this scaffolding to characterize the *shadow region* spanned by the agent in question. This area of the space blocked from view by an obstacle is in fact the region in which we do not allow the agent to jump. Further, we consider over-approximations which, at the price of being more conservative, allow for simpler coding of the constraints. We note that the hyperplane arrangement is not only a convenient way to describe the obstacles but also serves as support for the shadow area function (i.e., the structure of the shadow region remains constant over a fixed cell) which henceforth allows a piecewise description.

To put the previous constructions into a manageable form we use mixed integer programming Jünger et al. [2009], Reinl and von Stryk [2007]. The particularity is that we use the hyperplane arrangement construct to both simplify the formulation Prodan et al. [2012] and to exploit the piecewise nature of the shadow regions Stoican et al. [2014]. Through codification methods found in Vielma and Nemhauser [2011] we provide mixed integer constructs which describe both the shadow region and its complement in both exact and over-approximation forms. For the latter we arrive to a simplified form (involving only binary variables) which seems to be a generalization of results shown in Maia and Galvão [2009] and Richards and Turnbull [2015]. Lastly, we introduce these constraints into an MPC problem and verify that no corners are cut.

### 1.1 Notation

The collection of all possible combinations of $N$ binary variables is given by $\{0,1\}^N = \{(b_1,\dots,b_N) : b_i \in \{0,1\}, \forall i = 1\dots N\}$, the same definition holds for sign tuples $\{-,+\}^N$. $\text{Cone}(p,X) = \{p + \alpha(x-p), \forall x \in X, \forall \alpha \geq 0\}$ denotes the pointed cone with extreme point $p$ and tangent

to set $X$. $\text{Conv}(X,Y) = \{\alpha x + (1-\alpha)y, \forall x \in X, \forall y \in Y, 0 \leq \alpha \leq 1\}$ is the convex hull of the sets $X$ and $Y$.

## 2. PRELIMINARIES

Let us consider a finite collection of hyperplanes from $\mathbb{R}^n$, $\mathbb{H} = \{\mathcal{H}_i\}_{i\in\mathcal{I}}$ with

$$\mathcal{H}_i = \{x \in \mathbb{R}^n : \; h_i x = k_i\}, \; i \in \mathcal{I}, \tag{1}$$

where $\mathcal{I} \triangleq \{1 \dots N\}$ and $(h_i, k_i) \in \mathbb{R}^{1\times n} \times \mathbb{R}$.

Each of these hyperplanes partitions the space into two disjoint regions (which halve the space and hence are called "half-spaces"):

$$\mathcal{H}_i^+ = \{x \in \mathbb{R}^n : \quad h_i x \leq \quad k_i\}, \tag{2a}$$

$$\mathcal{H}_i^- = \{x \in \mathbb{R}^n : \; -h_i x \leq -k_i\}. \tag{2b}$$

Furthermore, hypeplanes (1) cut the space $\mathbb{R}^n$ into disjoint cells

$$\mathcal{A}(\sigma) = \bigcap_{i\in\mathcal{I}} \mathcal{H}_i^{\sigma(i)}, \tag{3}$$

which are feasible intersections of halfspaces (2a)–(2b) with the signs appropriately taken from the sign tuple $\sigma = (\sigma(1), \dots, \sigma(N))$. Such a partitioning of the space is called a hyperplane arrangement and is the union of all cells (3), that is, $\mathbb{R}^n = \mathbb{A}(\mathbb{H}) = \bigcup_{\sigma\in\Sigma} \mathcal{A}(\sigma)$ where $\Sigma \subset \{-,+\}^N$ denotes the collection of all tuples describing non-empty regions (3).

We can then partition the sign tuples into 'admissible' ($\sigma^\circ \in \Sigma^\circ$) and 'forbidden' ($\sigma^\bullet \in \Sigma^\bullet$) where $\Sigma^\circ \cap \Sigma^\bullet = \emptyset$ and $\Sigma^\bullet \cup \Sigma^\circ = \Sigma$. The latter subset describes the obstacles whereas the former describes the complement of the obstacle collection:

$$\mathbb{S} \triangleq \bigcup_{\sigma^\bullet\in\Sigma^\bullet} \mathcal{A}(\sigma^\bullet), \; \mathbb{R}^n \setminus \mathbb{S} \triangleq \bigcup_{\sigma^\circ\in\Sigma^\circ} \mathcal{A}(\sigma^\circ). \tag{4}$$

In addition, let us consider a point $x \in \mathbb{R}^n \setminus \mathbb{S}$. Then, the *shadow region* $\mathcal{B}(\mathbb{S}, x)$ given as in Strutu et al. [2013] is the collection of all the points from $\mathbb{R}^n \setminus \mathbb{S}$ which are not "visible" from '$x$':

$$\mathcal{B}(\mathbb{S}, x) = \{y \in \mathbb{R}^n : \quad [x,y] \cap \mathbb{S} \neq \emptyset\}. \tag{5}$$

This simply states that if the segment $[x,y]$ intersects $\mathbb{S}$ it means that point $x$ is "hidden" by obstacles $\mathbb{S}$ and therefore is not "visible" from the viewpoint of $x$.

Considering definition (4), region (5) is rewritten [1] as

$$\mathcal{B}(\mathbb{S}, x) = \bigcup_{\sigma^\bullet\in\Sigma^\bullet} \mathcal{B}(\sigma^\bullet, x). \tag{6}$$

To construct set (6) we have to deal with the parameter $x$. In order to do so, consider hereinafter the auxiliary construction

$$\mathcal{E}(\sigma^\bullet, x) = \mathcal{A}(\sigma^\bullet) \cap \left( \bigcup_{x\notin\mathcal{H}_i^{\sigma^\bullet(i)}} \mathcal{H}_i \right) \cap \left( \bigcup_{x\in\mathcal{H}_i^{\sigma^\bullet(i)}} \mathcal{H}_i \right), \tag{7}$$

which denotes the tangent points of $\mathcal{A}(\sigma^\bullet)$ from the viewpoint of $x$.

*Remark 1.* In $\mathbb{R}^2$, (7) reduces to a set of disconnected extreme points of the obstacle $\mathcal{A}(\sigma^\bullet)$. In general, in $\mathbb{R}^n$ we obtain a connected union of $n-1$ flats ("ridges"). ♦

[1] To shorten the notation, we write $\mathcal{B}(\mathcal{A}(\sigma^\bullet), x)$ in the compact form $\mathcal{B}(\sigma^\bullet, x)$.

*Proposition 2.* For any $x \in \mathcal{A}(\sigma^\circ)$ where $\sigma^\circ \in \Sigma^\circ$, the shadow region $\mathcal{B}(\sigma^\bullet, x)$ has a constant structure given by

$$\mathcal{B}(\sigma^\bullet, x) = \text{Cone}(x, \mathcal{E}(\sigma^\bullet, x)) \cap \bigcap_{\sigma^\circ(i)\neq\sigma^\bullet(i)} H_i^{\sigma^\bullet(i)} \tag{8}$$

where [2]

$$\mathcal{E}(\sigma^\bullet, \sigma^\circ) = \mathcal{A}(\sigma^\bullet) \cap \left( \bigcup_{\sigma^\circ(i)\neq\sigma^\bullet(i)} \mathcal{H}_i \right) \cap \left( \bigcup_{\sigma^\circ(i)=\sigma^\bullet(i)} \mathcal{H}_i \right) \tag{9}$$

*Proof.* By construction, the shadow area can be written as $\mathcal{B}(\sigma^\bullet, x) = \text{Cone}(x, \mathcal{A}(\sigma^\bullet)) \cap \bigcap_{x\notin H_i^{\sigma^\bullet(i)}} H_i^{\sigma^\bullet(i)}$. This becomes (8) if we note that the cone spanned from $x$ and tangent to $\mathcal{A}(\sigma^\bullet)$ is completely characterized by $x$ and $\mathcal{E}(\sigma^\bullet, x)$. Term (7) is rewritten in form (9) is we note that the indices for which $x \notin H_i^{\sigma^\bullet(i)}$ and $x \in H_i^{\sigma^\bullet(i)}$ remain the same for any point taken from $\mathcal{A}(\sigma^\circ)$ and are in fact given by checking whether the regions $A(\sigma^\bullet)$ and $A(\sigma^\circ)$ lie on the same (or opposite) sides of the i-th hyperplane. □

Proposition 2 shows that it suffices to compute a parametrized set for any $x$ in a given cell $\mathcal{A}(\sigma^\circ)$ and then replace the parameter $x$ with the actual value at run-time. While this reduces the computation burden, the formulation for the shadow area is still relatively difficult due to $\text{Cone}(x, \mathcal{E}(\sigma^\bullet, \sigma^\circ))$. A solution, as shown in the next corollary, is to consider an over-approximation of the shadow region.

*Corollary 3.* Let there be $\mathcal{B}(\sigma^\bullet, \sigma^\circ) = \bigcup_{x\in\mathcal{A}(\sigma^\circ)} \mathcal{B}(\sigma^\bullet, x)$ the shadow region associated to a feasible tuple $\sigma^\circ$. Then, this region depends only on $\sigma^\circ$ and is described as follows:

$$\mathcal{B}(\sigma^\bullet, \sigma^\circ) = \bigcap_{\sigma^\circ(i)\neq\sigma^\bullet(i)} H_i^{\sigma^\bullet(i)}, \tag{10}$$

*Proof.* From the definition of $\mathcal{B}(\sigma^\bullet, \sigma^\circ)$, the fact that $\bigcup_i (A_i \cap B) = (\bigcup_i A_i) \cap B$ and (8) follows that $\mathcal{B}(\sigma^\bullet, \sigma^\circ) = \bigcup_{x\in\mathcal{A}(\sigma)} \text{Cone}(x, \mathcal{E}(\sigma^\bullet, \sigma^\circ)) \cap \bigcap_{\sigma^\circ(i)\neq\sigma^\bullet(i)} H_i^{\sigma^\bullet(i)}$ which leads to (10). □

By using the over-approximation (10) the shadow region not only retains the same structure for any $x \in \mathcal{A}(\sigma^\circ)$ but actually remains constant. Hence, at run-time it is necessary only to identify the currently active tuple $\sigma^\circ$ and use the corresponding region (10).

*Remark 4.* In general, we may consider the blind area resulting from a set rather than from a point ($x \in \mathbf{X}$). The only difficulty is to check whether the set $\mathbf{X}$ stays in one or more of the regions (3). Defining $\Sigma_{\mathbf{X}} \triangleq \{\sigma \in \Sigma^\circ : \; \mathbf{X} \cap \mathcal{A}(\sigma) \neq \emptyset\} \subseteq \Sigma^\circ$ allows to characterize the shadow region:

$$\mathcal{B}(\sigma^\bullet, \mathbf{X}) = \bigcup_{x\in\mathbf{X}\cap\mathcal{A}(\sigma_x), \sigma_x\in\Sigma_{\mathbf{X}}} (\mathcal{B}(\sigma^\bullet, x)), \tag{11a}$$

$$\mathcal{B}(\sigma^\bullet, \Sigma_{\mathbf{X}}) = \bigcup_{\sigma_{\mathbf{X}}\in\Sigma_{\mathbf{X}}} \mathcal{B}(\sigma^\bullet, \sigma_{\mathbf{X}}). \tag{11b}$$

along the lines of Proposition 2 and Corollary 3. ♦

[2] To underline that the set depends only on $\sigma^\circ$ and not on any particular $x \in \mathcal{A}(\sigma^\circ)$ we changed from $\mathcal{E}(\sigma^\bullet, x)$ to $\mathcal{E}(\sigma^\bullet, \sigma^\circ)$.

*2.1 Illustrative example*

Consider the example depicted in Figure 1 with two obstacles in $\mathbb{R}^2$, $\mathbb{S} = S_1 \cup S_2$ defined by 5 hyperplanes. These partition the space into 16 cells from which 2 describe the obstacles and the rest characterize the feasible space $\mathbb{R}^2 \setminus \mathbb{S}$. More precisely, we identify $\Sigma^\bullet = \{\sigma_1, \sigma_2\}$ such that $S_1 = \mathcal{A}(\sigma_1)$ and $S_2 = \mathcal{A}(\sigma_2)$ for $\sigma_1 = (- - + + +)$ and $\sigma_2 = (+ - - + +)$. We apply now the shadow

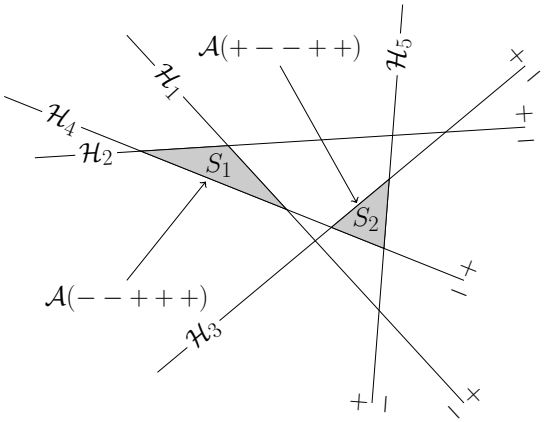


Fig. 1. Illustration of a collection of obstacles and their associated hyperplane arrangement.

region descriptions for $S_1$. In Figure 2 we take a point $x_1 \in \mathcal{A}(\sigma)$ for $\sigma = (+ + + + +)$. Checking the signs for

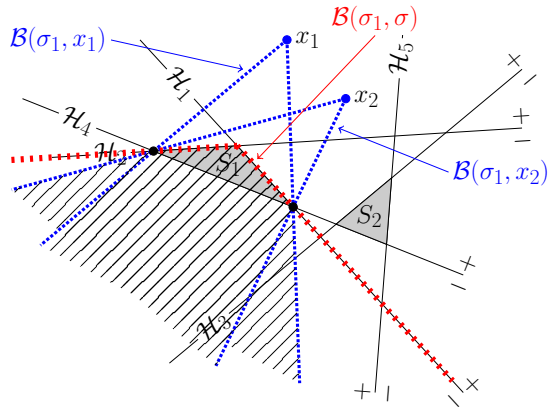


Fig. 2. Illustration of exact and over-approximated shadow regions.

tuples $\sigma_1$ and $\sigma$ we note that $x_1$ shares the same half-spaces with $S_1$ for indices 3, 4 and 5, the only different signs being at indices 1 and 2. Using this information in (7), or alternatively in (9), we note that the set of tangent points of $S_1$ from the viewpoint of $x_1$ consists of two points $\mathcal{E}(\sigma_1, x_1) = \{\mathcal{H}_2 \cap \mathcal{H}_4, \mathcal{H}_1 \cap \mathcal{H}_4\}$. Next, we can compute $\text{Cone}(x_1, S_1)$, which is the cone defined by the rays starting from $x_1$ and passing through $\mathcal{E}(\sigma_1, x_1)$. By adding the half-spaces separating the obstacle from the observation point $(\mathcal{H}_1^-, \mathcal{H}_2^-)$ we obtain the shadow region $\mathcal{B}(\sigma_1, x_1) = \text{Cone}(x_1, S_1) \cap \mathcal{H}_1^- \cap \mathcal{H}_2^-$. We depict in Figure 2 the over-approximation strategy employed in Corollary 3. That is, we take an additional point $x_2 \in \mathcal{A}(\sigma)$ from the same cell and depict the resulting shadow region $\mathcal{B}(\sigma_1, x_2) = \text{Cone}(x_2, S_1) \cap \mathcal{H}_1^- \cap \mathcal{H}_2^-$. Comparing with $\mathcal{B}(\sigma_1, \sigma) = \mathcal{H}_1^- \cap \mathcal{H}_2^-$, constructed as in Corollary 3, it can be seen that $\mathcal{B}(\sigma_1, \sigma)$ contains any region $\mathcal{B}(S_1, x)$ for $x \in \mathcal{A}(\sigma)$, and in particular for $x \in \{x_1, x_2\}$.

## 3. MIXED INTEGER REPRESENTATION

In Section 2 we gave various formulations for shadow regions observed from the point of view of an agent and with multiple obstacles. Regardless of the particular construction, the issue is that the resulting feasible region is non-convex (and in the case of multiple obstacles, not even connected) and the problem is nonlinear. Henceforth, we use mixed integer formulations, that is, we add to the original problem binary variables which help describe the problem in a pseudo-linear formulation.

As a first step, we define the mapping $\delta : \{-,+\}^N \times \{-,+\}^N \to \{0\} \cup [1, \infty)$:

$$\delta(\sigma_1, \sigma_2) = \sum_i \delta_i(\sigma_1, \sigma_2), \tag{12}$$

where $\delta_i(\sigma_1, \sigma_2) = \begin{cases} 1 - \sigma_2(i), & \sigma_1(i) = \text{`}+\text{'} \\ \sigma_2(i), & \sigma_1(i) = \text{`}-\text{'} \end{cases}$. We abuse the notation and whenever convenient (in the definition of (12) for example) we equate '-' with '0' and '+' with '1'. With this in mind, if follows that $\delta$ maps the difference between the two sign tuples $\sigma_1$ and $\sigma_2$: $\delta(\sigma_1, \sigma_2) = \begin{cases} 0, & \sigma_1 = \sigma_2 \\ \geq 1, & \sigma_1 \neq \sigma_2 \end{cases}$. Using constructions similar to the ones in Vielma and Nemhauser [2011] and the references therein the following representation of $\mathcal{B}(\sigma^\bullet, x)$ is provided.

*Proposition 5.* Let there be a point $x \in \mathcal{A}(\sigma)$ and an obstacle $\mathcal{A}(\sigma^\bullet)$. Then a point $x^+$ is inside $\mathcal{B}(\sigma^\bullet, x)$ iff

$$x^+ = x + \sum_j \beta_j (v_j - x), \tag{13a}$$

$$\sum_{j \text{ s.t. } v_j \notin \mathcal{E}(\sigma^\bullet, \sigma^\circ)} \beta_j \leq M \delta(\sigma^\circ, \sigma), \quad \forall \sigma^\circ \in \Sigma^\circ, \tag{13b}$$

$$\beta_j \geq 0, \tag{13c}$$

$$\sigma^\bullet(i) h_i x^+ \leq \sigma^\bullet(i) k_i + M(1 - \delta_i(\sigma^\bullet, \sigma)), \tag{13d}$$

where $v_j$ denote the extreme points of the obstacle.

*Proof.* Equations (13a) and (13c) describe a cone spanned from $x$ and with rays $v_j$. (13b) ensures that only the extreme points active for the current cell $\mathcal{A}(\sigma)$ participate in the cone construction (since the terms $\beta_j$ are positive, if their sum is zero then each term is zero). Lastly, (13d) adds to the mix the half-spaces which separate the obstacle from the point $x$, as required by definition (8). □

*Remark 6.* The above equations make use of the "big M" representation. That is, we consider in the right hand side a combination of binary variables multiplied by a large value (i.e., 'M'). This means that whenever the binary part is '$\geq 1$' the right hand is practically 'infinite' thus making the associated inequality redundant. In particular, in Proposition 5 the current location of point $x$ (i.e, its sign tuple $\sigma$) is unknown. Consequently we enumerate all the feasible tuples in (13b), and, iff $\sigma \neq \sigma^\circ$ the associated inequality is neglected. ♦

In Proposition 5 we provided a mixed integer description of the shadow area. However, if we wish to describe the feasible region, we need its complement.

*Proposition 7.* Let there be a point $x \in \mathcal{A}(\sigma)$ and an obstacle $\mathcal{A}(\sigma^\bullet)$. Then a point $x^+$ is outside $\mathcal{B}(\sigma^\bullet, x)$ iff

$$M(1-\alpha) \geq |x^+ - x - \sum_j \beta_j (v_j - x)|, \tag{14a}$$

$$|\beta_j| \leq M\delta(\sigma^\circ, \sigma),\ \forall j \text{ s.t. } v_j \notin \mathcal{E}(\sigma^\bullet, \sigma^\circ), \tag{14b}$$

$$\beta_j \leq M(1-\gamma_j), \tag{14c}$$

$$\gamma_j \leq \delta(\sigma^\circ, \sigma), \forall j \text{ s.t. } v_j \notin \mathcal{E}(\sigma^\bullet, \sigma^\circ), \tag{14d}$$

$$\sum_j \gamma_j > 0, \tag{14e}$$

$$-\sigma^\bullet(i) h_i x^+ \leq -\sigma^\bullet(i) k_i + M[\delta_i(\sigma^\bullet, \sigma) + \alpha + \rho_i], \tag{14f}$$

$$N > \sum_i \left[\rho_i + \delta_i(\sigma^\bullet, \sigma)\right], \tag{14g}$$

for any $\sigma^\circ \in \Sigma^\circ$ and with $\alpha, \gamma_j, \rho_i \in \{0,1\}$ auxiliary binary variables.

*Proof.* Using (8) and the fact that $\overline{A \cap B} = \overline{A} \cup \overline{B}$ we have that $\overline{\mathcal{B}(\sigma^\bullet, x)} = \overline{\text{Cone}\,(x, \mathcal{E}(\sigma^\bullet, x))} \cup \bigcup_{\sigma^\circ(i) \neq \sigma^\bullet(i)} H_i^{\sigma^\circ(i)}$. Binary variable $\alpha$ selects between $\overline{\text{Cone}\,(x, \mathcal{E}(\sigma^\bullet, x))}$ and $\bigcup_{\sigma^\circ(i) \neq \sigma^\bullet(i)} H_i^{\sigma^\circ(i)}$, $\rho_i$ which appear in (14f), (14g) select one of the half-spaces $H_i^{\sigma^\circ(i)}$. The rest of the constraints, (14b)–(14e) describe the complement of the cone: (14a) describes a cone spanned from $x$ and with rays $v_j$ and (14b) lets only the extreme points active for the current sign tuple to participate in the cone construction; (14e) with (14d) ensure that at least one of the active coefficients $\gamma_j$ is equal to one (and hence that at least a $\beta_j$ is negative thus ensuring that we are outside of the cone). □

*Remark 8.* In both Proposition 5 and 7 we considered only one obstacle (the one defined by tuple $\sigma^\bullet$). The extension to the case of multiple obstacles is straightforward. For the shadow area additional binary variables need to be considered in order to describe the union of shadow regions resulting from each of the obstacles. On the other hand, to describe the visible region, we simply intersect the regions obtained in (14a)–(14g): $x \notin \bigcup_{\sigma^\bullet \in \Sigma^\bullet} B(\sigma^\bullet, x)$ is equivalent with $x \in \overline{\bigcup_{\sigma^\bullet \in \Sigma^\bullet} B(\sigma^\bullet, x)} \Leftrightarrow x \in \bigcap_{\sigma^\bullet \in \Sigma^\bullet} \overline{B(\sigma^\bullet, x)}$. ♦

The exact formulations (13a)–(13d) and (14a) –(14g) are complex due to the presence of term $\text{Cone}(\sigma^\bullet, x)$. If on the other hand we use the over-approximation of Corollary 3, we greatly simplify the representations.

*Proposition 9.* Assume that the current position is $x \in \mathcal{A}(\sigma)$ and that the obstacle is $\mathcal{A}(\sigma^\bullet)$. Then the future position $x^+ \in \mathcal{A}(\sigma^+)$ is constrained as follows:

(i) for $x^+ \in \mathcal{B}(\sigma^\bullet, \sigma)$:

$$\sum_i \delta_i(\sigma^\bullet, \sigma) \cdot \delta_i(\sigma^\bullet, \sigma^+) = 0, \tag{15}$$

(ii) for $x^+ \notin \mathcal{B}(\sigma^\bullet, \sigma)$:

$$\sum_i \delta_i(\sigma^\bullet, \sigma) \cdot \delta_i(\sigma^\bullet, \sigma^+) > 0, \tag{16}$$

*Proof.* For both cases it is a matter of ignoring the constraints related to the term $\text{Cone}(\sigma^\bullet, x)$ which means that we remain with (13d) and (14f)–(14g), respectively. Further, we interpret these constraints in terms of three sign tuples: $\sigma^+$ characterizes the shadow/visible region and is constrained by the current position ($\sigma$) and the obstacle ($\sigma^\bullet$). We limit $\sigma^+$ to describing: the regions defined only by the half-spaces which separate between the obstacle and the current position.

This constraint is expressed by $\delta_i(\sigma^\bullet, \sigma) \cdot \delta_i(\sigma^\bullet, \sigma^+) = 0$: whenever $\sigma^\bullet(i)$ and $\sigma(i)$ share the same sign (i.e., $\delta_i(\sigma^\bullet, \sigma) = 0$) the value of $\sigma^+(i)$ is not constrained; whenever $\sigma^\bullet(i)$ and $\sigma(i)$ have opposite signs (i.e., $\delta_i(\sigma^\bullet, \sigma) = 1$) we have that $\sigma^+(i)$ is constrained to have the same sign as $\sigma^\bullet(i)$ (thus making $\delta_i(\sigma^\bullet, \sigma^+) = 0$).

Depending which region we wish to describe (shadow or visible region) we reach (15) or (16). For case (i), forcing the equality means that each of the terms of the sum is zero (since we have a sum of positive terms). To describe case (ii) it suffices that at least one of the terms of the sum is non-zero. Since each of the sum terms is positive, the fact that the sum is positive means that at least one of them is positive. □

In Proposition 9 the constraints (15)–(16) are linear only if $\sigma$ is known. If $\sigma$ is itself a variable we have bilinear binary terms which make any optimization problem into which they appear MINLP. Needless to say, this should be avoided at all costs. The solution is to provide a piecewise description which, through an increase in the number of constraints, keeps the formulation linear.

*Corollary 10.* Assume that the obstacle is $\mathcal{A}(\sigma^\bullet)$. Then the future position $x^+ \in \mathcal{A}(\sigma^+)$ is constrained as follows:

(i) for $x^+ \in \mathcal{B}(\sigma^\bullet, \sigma)$:

$$\sum_i \delta_i(\sigma^\bullet, \sigma^\circ) \cdot \delta_i(\sigma^\bullet, \sigma^+) \leq N\delta(\sigma^\circ, \sigma), \tag{17}$$

(ii) for $x^+ \notin \mathcal{B}(\sigma^\bullet, \sigma)$:

$$\sum_i \delta_i(\sigma^\bullet, \sigma^\circ) \cdot \delta_i(\sigma^\bullet, \sigma^+) > -N\delta(\sigma^\circ, \sigma), \tag{18}$$

for all $\sigma^\circ \in \Sigma^\circ$.

*Proof.* We write the equations (15)–(16) for each of the feasible sign tuples $\sigma^\circ \in \Sigma^\circ$. Further, recall that $\delta(\sigma^\circ, \sigma)$ is $\geq 1$ iff $\sigma^\circ \neq \sigma$. It follows that out of the equations (17)–(18) only the ones corresponding to the active sign tuple remain and the rest are ignored (as they are always true, regardless of the left-hand side value). □

### *3.1 Illustrative example*

We consider the example from Section 2 and recall that the shadow region spanned from point $x_1$ with respect to obstacle $S_1 = \mathcal{A}(\sigma_1)$ was found to be:

$$\mathcal{B}(\sigma_1, x_1) = \text{Cone}(x_1, S_1) \cap \mathcal{H}_1^- \cap \mathcal{H}_2^-.$$

Using Proposition 5 we obtain the following mixed integer formulation (as seen in Figure 3, the extreme points of $S_1$ are denoted as $v_1, v_2, v_3$):

$$
\begin{aligned}
x^+ &= x + \beta_1(v_1 - x) + \beta_2(v_2 - x) + \beta_3(v_3 - x),\\
&\dots\dots\\
\beta_3 &\le M\left(5 - \sigma(1) - \sigma(2) - \sigma(3) - \sigma(4) - \sigma(5)\right),\\
&\dots\dots\\
\beta_1 &\ge 0,\ \beta_2 \ge 0,\ \beta_3 \ge 0,\\
-h_i x^+ &\le -k_i + M(1 - \sigma(i)),\ i \in \{1,2\}\\
h_i x^+ &\le \ \ k_i + M\sigma(i),\ i \in \{3,4,5\}
\end{aligned}
$$

We observe that the cone can be composed from at most three rays (the extreme points of $S_1$). Which of these is active is governed by equations (13b). For compactness reasons we consider here only the case $\sigma^\circ = (+ + + + +)$. The last five constraints show which of the half-spaces of the obstacle remain active in the shadow region representation. Consider that in the above equations $\sigma$ is replaced with $\sigma^\circ$. The following effects can be observed: 1) the right side of the third equation becomes zero and hence $\beta_3 = 0$ which means that the cone formulation becomes $x^+ = x + \beta_1(v_1 - x) + \beta_2(v_2 - x)$; 2) out of the half-space constraints we remain with only $-h_1 x^+ \le -k_1$ and $-h_2 x^+ \le -k_2$. We can then conclude that by choosing $\sigma^\circ$ we retrieve the shadow region $\mathcal{B}(\sigma_1, x_1)$.

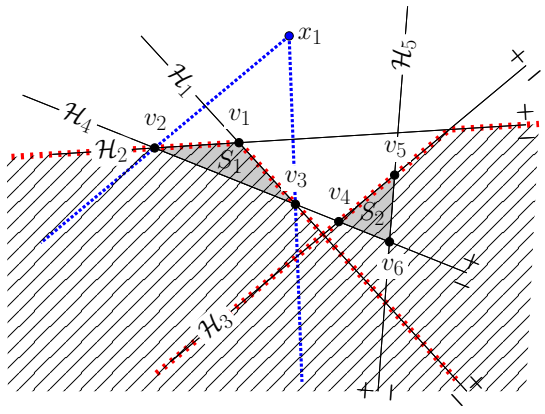


Fig. 3. Illustration of over-approximated shadow regions in a multi-obstacle environment.

Proposition 7 has a similar construction as the one provided in the above illustrative example, hence we skip to the over-approximate representations given in Proposition 9. We consider $\mathcal{B}(\sigma^\bullet, \sigma^\circ)$ with the sign tuples defined as in (10). Then, the shadow region inclusion constraint is given as:

$$\sigma^+(1) + \sigma^+(2) = 0,$$

and the shadow region exclusion constraint as

$$\sigma^+(1) + \sigma^+(2) > 0.$$

This can be easily checked in Figure 3. From the first equations we have that $x^+$ can lie in any region which respects $\sigma^+(1) = \sigma^+(2) = \text{`}-\text{'}$, in other words $x^+ \in \mathcal{H}_1^- \cap \mathcal{H}_2^-$ whereas the second equation imposes the opposite, that $x^+$ cannot lie in any region which respects simultaneously both $\sigma^+(1) = \sigma^+(2) = \text{`}-\text{'}$, hence that $x^+ \notin \mathcal{H}_1^- \cap \mathcal{H}_2^-$. These constraints can easily manipulate multiple obstacles: the patterned region from Figure 3 describes the over-approximate shadow region spanned from $x_1$ with respect to obstacles $S_1$ and $S_2$. Constraints:

$$\sigma^+(1) + \sigma^+(2) > 0,\ \sigma^+(2) + \sigma^+(3) > 0.$$

describe the feasible space in which $x^+$ can lie. The extension to Corollary 10 is straightforward and thus not exemplified here.

### *3.2 Comparison with the state of the art*

Since the paper aims to provide an exact description of the shadow region we investigate the proposed approach through comparison with the state of the art. Specifically, we refer to Maia and Galvão [2009] and Richards and Turnbull [2015], where it appears that barring a change in notation, constraints involving binary variables are of the same type as in Corollary 10. That is, Maia and Galvão [2009] imposes a similar set of constraints in the over-approximate case while Richards and Turnbull [2015] considers a subset of these constraints (as it limits their variation along the prediction horizon). Several remarks are to be made. Foremost is that the constructions shown in these papers consider as obstacle a single polyhedral set whereas the approach proposed here considers arbitrarily many obstacles. And although their formulation can be generalized to also include arbitrarily many obstacles, it appears that the constraint design is not fully exploited. For example, the obstacle is defined as the intersection of the '+' side of its support hyperplanes, hence, it is not clear how the constraints would be written in the more general case. It is also worth noting that the number of binary variables depends on both the number of obstacles and their complexity, while in our approach the number of binary variables remains fixed (as the obstacles are characterized by forbidden sign tuples).

## 4. MPC IMPLEMENTATION

Up to this point the paper mainly discussed the geometric interpretation and the mixed integer formulation of the shadow region (and its complement). Next, the proposed novel description is integrated within an MPC framework since it deals natively with constraints and is thus, well suited for obstacle avoidance control problems. Assuming, as it reasonable to do for small sampling times, that in a sampling interval an agent moves along a straight line we can avoid cutting the corner of an obstacle by forcing the next position of the agent to be outside of the shadow region spanned by the current position and the obstacle(s). In fact, for an LTI dynamic given as

$$x_{k+1} = Ax_k + Bu_k,\ y_k = Cx_k \tag{19}$$

we impose that $y_{k+1} \notin \bigcup_{\sigma^\bullet \in \Sigma^\bullet} \mathcal{B}(\sigma^\bullet, y_k)$ – or its over-approximation counterpart $\mathcal{B}(\sigma^\bullet, \sigma_k)$ – in addition to the usual constraints[3] (e.g., $y_k \in \mathcal{Y}$, $u_k \in \mathcal{U}$). The sign tuple $\sigma_{k+i}$ characterizing the predicted output $y_{k+i}$ is itself a variable and cannot be assumed as a constant. Here we make use of the previous sections where we have provided piecewise descriptions of the shadow regions (either through Proposition 7 or Corollary 10). With these constructs we can now formulate the optimization problem and solve it:

[3] With $N_p$ the prediction horizon, $Q$ and $R$ the positive definite weighting matrices.

$$u^* = \arg \min_{u_k, \sigma_{k+1}, \ldots u_{k+N_p-1}, \sigma_{k+N_p}} \sum_{i=0}^{N_p-1} \|x_{k+i+1}\|_Q + \|u_k\|_R, \tag{20a}$$

$$\text{s.t.} x_{k+i+1} = Ax_{k+i} + Bu_{k+i}, \tag{20b}$$

$$y_{k+i} \in \mathcal{Y},\ u_{k+i} \in \mathcal{U}, \tag{20c}$$

$$y_{k+i+1} \notin \bigcup_{\sigma^\bullet \in \Sigma^\bullet} \mathcal{B}(\sigma^\bullet, \sigma_{k+i}), \quad i = 1 \ldots N_p. \tag{20d}$$

The result is an MILP problem which requires specialized solvers (CPLEX, Gurobi, etc) but which can be handled relatively easy.

We proceed to do so for the dynamics used for UAV path planning in Grøtli and Johansen [2012], Grancharova et al. [2014] of the form (19):

$$x_{k+1} = \begin{bmatrix} I_2 & I_2 \\ 0_2 & I_2 \end{bmatrix} x_k + \begin{bmatrix} 0_2 \\ I_2 \end{bmatrix} u_k,\ y_k = [I_2\ 0_2]\, x_k, \tag{21}$$

which is a discretized integrator with sampling time $\Delta t = 1$, the state is composed from position and velocity and the output is the agent's position. For the MPC problem we choose $Q$ and $R$ as identity matrices, a prediction horizon $N_p = 10$ and output, and respectively, input constraints of form $\mathcal{Y} = \{y :\ |y| \leq [8\ 8]^\top\}$ and $\mathcal{U} = \{u :\ |u| \leq 0.25\}$.

The result of simulating with starting coordinates $x_0 = [6.07\ 2.09\ 0\ 0]^\top$ and using the shadow region exclusion constraints from Corollary 10 is the trajectory (dotted blue line) depicted in Figure 4. Note that the constraints apply only to the position component of the state. For comparison, we simulate from the same starting point without the corner cutting constraints (i.e., (20d)) and impose only obstacle avoidance constraints (dashed red line). As expected, we observe that the addition of corner cutting constraints leads to a trajectory which avoids intra-sample obstacle collision.

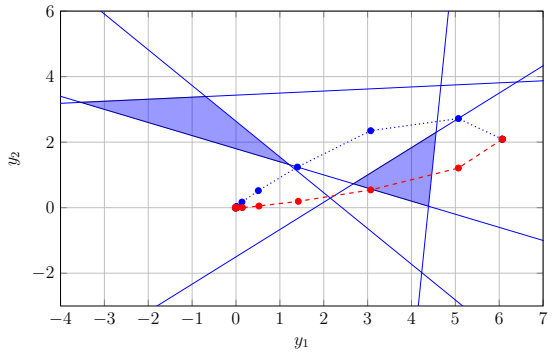


Fig. 4. Illustration of corner cutting simulation.

## 5. CONCLUSIONS

This paper proposed an in depth analysis of the corner cutting problem and provided a framework which can handle a multi-obstacle environment. Both exact and over-approximation constructs for the shadow region have been given. Moreover, we have shown that the mapping of such a region is piecewise with the support generated by a hyperplane arrangement. Mixed integer formulations have been considered and compared with the state of the art. We employed the theoretical results in an MPC scheme and have shown through simulations the desired obstacle avoidance behavior.

**Acknowledgment.** This work has been partially funded by the Sectorial Operational Programme Human Resources Development 20072013 of the Ministry of European Funds through the Financial Agreement [grant number POSDRU/159/1.5/S/132395] and by a grant of the Romanian National Authority for Scientific Research, CNCS - UEFISCDI, project identification number PN-II-ID-PCE-2011-3-0235.

## REFERENCES

R. Deits and R. Tedrake. Efficient mixed-integer planning for UAVs in cluttered environments. In *Proc. of IEEE Int. Conf. on Robotics and Automation*, 2015.

A. Grancharova, E. I. Grøtli, D.-T. Ho, and T. A. Johansen. UAVs trajectory planning by distributed MPC under radio communication path loss constraints. *Journal of Intelligent and Robotic Systems*, 2014. doi: 10.1007/s10846-014-0090-1.

E. I. Grøtli and T. A. Johansen. Path planning for UAVs under communication constraints using SPLAT! and MILP. *Journal of Intelligent and Robotic Systems*, 65 (1-4):265–282, 2012. doi: 10.1007/s10846-011-9619-8.

M. Jünger, M. Junger, T.M. Liebling, D. Naddef, G. Nemhauser, and W.R. Pulleyblank. *50 Years of Integer Programming 1958-2008: From the Early Years to the State-of-the-Art*. Springer Verlag, 2009.

M. H. Maia and R. K. H. Galvão. On the use of mixed-integer linear programming for predictive control with avoidance constraints. *Int. J. Robust Nonlinear Control*, 19:822–828, 2009. doi: 10.1002/rnc.1341.

I. Prodan, F. Stoican, S. Olaru, and S.I. Niculescu. Enhancements on the Hyperplanes Arrangements in Mixed-Integer Techniques. *Journal of Optimization Theory and Applications*, 154(2):549–572, 2012. ISSN 0022-3239. doi: 10.1007/s10957-012-0022-9.

C. Reinl and O. von Stryk. Optimal control of multi-vehicle-systems under communication constraints using mixed-integer linear programming. In *Proc. of the 1st Int. Conf. on Robot comm. and coordination*, 2007.

A. Richards and O. Turnbull. Inter-sample avoidance in trajectory optimizers using mixed-integer linear programming. *Int. J. Robust Nonlinear Control*, 25:521–526, 2015. doi: 10.1002/rnc.3101.

F. Stoican, I. Prodan, M. I. Struţu, and D. Popescu. Geometrical interpretation on the coverage problems for a mobile agent. In *Proc. of the 18th Int. Conference on System Theory, Control and Computing*, pages 791–796, 2014.

M.-I. Strutu, F. Stoican, I. Prodan, D. Popescu, and S. Olaru. A characterization of the relative positioning of mobile agents for full sensorial coverage in an augmented space with obstacles. In *Proc. of the 21st Mediterranean Conf. on Control and Automation*, pages 936–941, 2013.

J.P. Vielma and G.L. Nemhauser. Modeling disjunctive constraints with a logarithmic number of binary variables and constraints. *Mathematical Programming*, 128 (1):49–72, 2011.